Upper-tropospheric troughs and North American monsoon rainfall in a long-term track dataset

Matthew R. Igel[1], Paul A. Ullrich[1,2], William R. Boos[2,3]

[1]Department of Land, Air and Water Resources, University of California Davis, Davis, 95616, USA

[2] Climate and Ecosystem Sciences Division, Lawrence Berkeley National Laboratory, Berkeley, 94720, USA

[3] Department of Earth and Planetary Science, University of California Berkeley, Berkeley, 94720, USA

Correspondence to: Matthew Igel (migel@ucdavis.edu)

Key Points:

- Upper-tropospheric troughs over southwest North America are identified in an atmospheric reanalysis, yielding a 40-year track dataset.
- Tropical upper-tropospheric troughs weakly but negatively affect North American Monsoon precipitation intensity in the trough center.
- When composited along the TUTT track, enhanced precipitation falls outside the main TUTT circulation.

Abstract. The North American monsoon is frequently affected by transient, propagating upper tropospheric vorticity anomalies. Sometimes called Tropical Upper-Tropospheric Troughs (TUTTs), these features have been claimed to episodically enhance monsoon rainfall. Here we track long-lived TUTTs in 40 years of reanalysis data, producing composites and case studies from 340 TUTTs which last, on average, seven days as they move westward across the North American monsoon region. TUTTs are thought to form from midlatitude Rossby wave breaking; case studies from our dataset support this theory. TUTTs move westward within the easterly upper-level flow in which they are embedded. In vortex-centered composites along the full tracks of long-lived TUTTs, we find no detectable increase in rainfall within the main TUTT circulation. Instead, negative precipitation anomalies lie within about 500 km of the TUTT center. Quasi-geostrophic ascent occurs in the southeast quadrant of TUTTs but is confined to the upper troposphere and does not appear to interact with precipitation. Positive anomalies of ascent and rainfall occur south and southeast of TUTTs but lie outside the main TUTT vortex, perhaps indicating concurrent variations in nearby climatological precipitation maxima. In contrast with previous case studies and subjective analyses that showed TUTTs enhance precipitation in parts of northwestern Mexico, our composites along the tracks of long-lived TUTTs portray these systems, to first order, as strong vorticity anomalies trapped in the upper troposphere that interact only weakly and indirectly with precipitation.

1. Introduction

In all monsoon climates, the region of peak seasonal mean precipitation lies on the equatorial side of an upper-level anticyclone. Mid- to upper-level vorticity anomalies that are both carried by and draw energy from this anticyclonic flow have been clearly documented in the South Asian monsoon (Hsu & Plumb, 2000; Krishnamurti & Bhalme, 1976; Ortega et al., 2017) and the North American monsoon (NAM) (Bieda et al., 2009; Newman & Johnson, 2012; Pytlak et al., 2005). These transient vorticity anomalies, in turn, interact with the background vertical shear and the moisture field in ways that have been claimed to alter regional precipitation.

For the North American monsoon in particular, westward-propagating upper-tropospheric disturbances are the most frequently occurring transient synoptic feature. They exist on nearly half of the days in an average summer season and are believed to contribute 20-25% of total summer precipitation in northern Mexico (Douglas & Englehart, 2007b). They are often called inverted troughs (IVs) or tropical upper-tropospheric troughs (TUTTs), named for the local minimum in geopotential that can be open to the equator and is typically most prominent between 200-500 hPa (Kelly & Mock, 1982; Newman & Johnson, 2012).

Despite the prevalence of TUTTs and their claimed contribution to the bulk water budget of the NAM region, many of the details of their induced precipitation patterns are unknown. For a cluster of rain gauges in northwestern Mexico, Douglas and Englehart (2007b) documented peak rainfall occurring west of the minimum 500 hPa geopotential in a 35-year climatology of IVs developed from weather maps (the west side of the TUTT would be the leading edge of the westward-propagating disturbance). In contrast, Pytlak et al. (2005) argued, based on case studies from the 2003-2004 North American Monsoon Experiment (NAME) (Higgins et al., 2006), that precipitation occurred on both the western and eastern sides of TUTTs, primarily due to the organization of mesoscale convective systems (MCSs) in those regions. Whitfield and Lyons (1992) found peak precipitation in the southeast quadrant of a TUTT but did so with only one case study over Texas, which is itself well to the east of the NAM region.

Some of these discrepancies in the location of peak precipitation relative to the TUTT center were reconciled by Finch and Johnson (2010), who performed detailed analyses of the quasi-geostrophic (QG) motion in one TUTT that was well-observed during the NAME field campaign. They found synoptic descent to the west of that TUTT was forced by thermal advection but that, despite this QG subsidence, topographic forcing resulted in enhanced convection in that region. This picture was refined by Newman and Johnson (2012), who argued, based on constrained cloud-resolving simulations of the same 2004 case study, that the TUTT enhanced CAPE and layer shear over the Sierra Madre mountain range. These findings, which suggest TUTTs prime an environment so that mesoscale processes can produce precipitation, are distinct from the earlier suggestion by Pytlak et al. (2005) that forcing for MCSs and precipitation was synoptic.

While much of our understanding of TUTTs has come from case studies, especially of NAME-year features (Finch & Johnson, 2010; Newman & Johnson, 2012; Pytlak et al., 2005), there have been several systematic attempts to identify TUTTs in observational data. As mentioned above, Douglas and Englehart (2007b) produced a 35-year analysis of transients moving across northern Mexico, though this was based primarily on manual inspection of surface and 500 hPa daily weather maps and likely included a wide variety of westward-propagating mid- and lower-tropospheric features in their IV category. They suggested that precipitation was enhanced to the east and west of the TUTT center. An empirical orthogonal function analysis of NAM synoptic variability in eight years of satellite-derived precipitation and reanalysis data showed that QG lifting around TUTTs plays a negligible role in organizing precipitation, with TUTT-induced vertical shears causing MCSs to form northwest of the TUTT center (Seastrand et al. 2015). Bieda et al. (2009) identified TUTTs from 1980-2002 in the North American Regional Reanalysis (NARR), finding an enhancement of total moisture in the NAME region and an enhancement of the amplitude of the diurnal cycle of lightning activity on days with TUTTs. Lahmers et al. (2016) found a long-term (1951-2010) increase in northern NAM TUTT track density in downscaled WRF simulations forced with the NCEP-NCAR reanalysis (Kalnay et al., 1996). Luong et al. (2017) found a long-term increase in atmospheric moisture and convective instability in simulations of historical severe weather events during the TUTT season. Together, these studies suggest a weak but consistent enhancement of regional precipitation from TUTTs in northwestern Mexico.

Additionally, some studies have pointed to important indirect effects of TUTTs on precipitation in the NAM. Rogers and Johnson (2007) and Johnson et al. (2007) suggested that TUTTs may be important contributors to the initiation of moisture surges in the Gulf of California, from which further circulations and convection may later develop.

The goal of this study is to create a dataset of time-resolved North American monsoon TUTT tracks (not just maps of climatological track density) in multiple decades of a modern reanalysis, then to use those tracks to improve understanding of TUTT structure and precipitation. One of our most rudimentary objectives is to validate the summary by Newman and Johnson (2012) that NAM TUTTs "are unique because they have enhanced precipitation on the western side ... while TUTTs throughout the rest of the world typically have enhanced precipitation on the eastern flank." In fact, we will show that this statement is not generally true along the entire track of long-lived TUTTs in the Central American domain, and the 2004 case studies that dominated such thinking may be anomalies in the longer climatology of NAM

TUTTs, unless the ERA5 reanalysis used here is somehow anomalous in its representation of the 2004 monsoon season. On a more detailed level, we seek to understand the mechanisms by which a TUTT alters precipitation, reconciling, if possible, the arguments by several prior studies that QG lifting is important (Pytlak et al. 2005) with those that find it is negligible in magnitude and thus insignificant compared to the effect TUTTs have on MCS formation through their influence on the environmental vertical shear (Newman and Johnson 2012, Seastrand et al. 2015). Our methodology contrasts strongly with that of prior work that has focused on case studies of small numbers of TUTTs over particular regions of Mexico (Pytlak et al. 2005, Newman and Johnson 2012) or that has used subjective identification of troughs based on criteria that include a variety of middle- and lower-tropospheric disturbances (Douglas and Englehart 2007). We seek to paint a picture of strong, long-lived NAM TUTTs along the entire length of their track.

This paper is organized as follows. First, we detail our methodology for identification and tracking of TUTTs. Our catalogue of TUTTs then enables us to describe their genesis and meteorology, their properties beginning with their dry dynamics, their moisture structure, and finally their associated mechanisms for precipitation production. These results are then summarized together with conclusions.

2. Identification and Tracking

We used TempestExtremes (Ullrich et al., 2021; Ullrich & Zarzycki, 2017) to track TUTTs. TempestExtremes is a flexible software package for identifying and tracking meteorological features in time and space in historical or simulated datasets. We used three search criteria to track TUTTs – 1) a 200 hPa stream function-indicated cyclonic rotation center (i.e. local minimum) with 2) no greater than a 325 m rise from the center over 1° in the 1000 hPa height field and 3) selection of only the strongest local minima within 5° great circle distance (see §6). The first criterion helped us locate rotational upper-tropospheric disturbances at a level where they are considered to be the strongest (Kelly & Mock, 1982). The second criterion was added to prevent surface-based meteorological phenomena (e.g. tropical cyclones) from entering the dataset. We estimated appropriate parameter values for the second criterion from Zarzycki and Ullrich (2017). These criteria were applied to 40 years of hourly ERA5 (Hersbach et al., 2020) reanalysis (1979 to 2018) at 0.25° x 0.25° spacing. The criteria were designed to be general and applicable to other reanalyses or forecast datasets at high enough resolution to resolve synoptic-scale features like TUTTs. We tracked upper-tropospheric cyclonic disturbances between 15°N to 40°N and 90°W to 120°W (visible area in Fig. 1 and highlighted in Fig. 3). July and August are the months of peak rainfall in the NAM (Adams & Comrie, 1997) and in potential vorticity (PV) streamer activity in the North Atlantic (Papin et al., 2020). So, we chose to only track entities that have at least some period of their track in July or August but which may originate or dissipate outside those months. We require that tracked disturbances last at least 2.75 days (see below) to be considered long-lived.

These tracking criteria result in 340 upper tropospheric disturbances which we will call TUTTs. They last up to 261 hours (see Fig. 2 next section) and 92% track from east to west across the domain. TUTT genesis does not occur preferentially at any time of day (not shown) which is consistent with a synoptic feature rather than one driven by diurnally forced convection. Figure 1a shows the number of hours with a TUTT track center in each 0.25° x 0.25° box (i.e. track density) over the 40 years of ERA5. Most TUTT centers occur east of the Sierra Madre Occidental and south of 30°N. There is a secondary maximum of occurrence over and to the west of the southern tip of the Baja California peninsula. Figure 1b provides a sense of the motion of TUTTs for locations with at least 50 TUTT centers. Motion is broadly toward the west and northwest at ~5 m s^{-1} with some local geographic influences to the pattern.

As a way of assessing our tracking method, we compare our TUTTs with those subjectively identified during the NAME year by Pytlak et al. (2005). Table 1 lists the dates of these TUTTs, including the numbered labels from Pytlak et al. (2005). We identify fewer TUTTs than Pytlak et al. (2005), but our TUTTs correspond well to disturbances they identify. Our identification method is intentionally strict since we are concerned with understanding TUTT behavior rather than quantifying all their possible impacts. Table 1 suggests a consequence of that choice is that we only identify a subset of all possible TUTTs but that we have a low false positive rate (only 1 potential false positive in the NAME year). It is possible that some of the TUTTs identified by Pytlak et al. (2005) do not pass the minimum time requirement to be included in our dataset. Our minimum longevity of 2.75 days was originally chosen because the TUTTs hand-selected by Pytlak et al. (2005) all spanned at least three days, but minimum longevities of slightly longer than 2 days or slightly shorter than 3 days would also be consistent. Regardless, TempestExtremes does a good job strictly identifying and tracking TUTTs.

In search of all the hand-analyzed TUTTs in Table 1, we also tested the capabilities of TempestExtremes by relaxing our search criteria to merge circulation centers within only 3° (rather than 5°) and by imposing a minimum longevity of either 0.75 days or 1.75 days. The resulting permissive TUTT dataset employing the shortest time limit includes 1373 feature tracks (quadruple our control count) across the 40 years of ERA5 data with some features on each of the days in Table 1 (“Permissive” column) as well as 23 other feature tracks in the NAME year. But the median feature longevity is just 36 hours and the dataset averages one identified TUTT on nearly every day within the search domain over the 40 July-August periods. Additionally, at 152 different times, there are as many as four features tracked simultaneously in our relatively small search domain. For comparison, the TUTT control dataset we use never includes more than one feature at a time. The 1.75-day limit yields 607 possible TUTTs (70% more than our control count) with a median longevity of 72 hours and up to three features tracked simultaneously. This dataset captures one more numbered TUTT in Table 1 than the control dataset, but that TUTT (number 6) is split into three features, and there are additionally five potential false positives. Such properties make these permissive datasets more inclusive of possible TUTTs (a desirable feature) but also more inclusive of possible spurious transient features (not in keeping with our goals). So, we proceed with using our strictest track dataset and note that our results should be considered in light of these relatively strict criteria.

Table 1 also includes hand-analyzed TUTTs that resulted in heavy precipitation events in the Lake Mead basin (Sierks et al., 2020) which is in the northwest corner of our search domain. Our dataset contains five of their eight identified TUTTs. Again, given our strict criteria this is an encouraging success rate. Sierks et al. (2020) examined 40 intense rainfall events in the Lake Mead basin in the past 40 years. Of those, 9 were related in some way to a tropical cyclone. These would not be expected to be associated with TUTTs, and indeed, our dataset does not include any of these dates. This helps confirm the contrapositive that TempestExtremes does not include tropical cyclone-associated events in the TUTT dataset.

3. TUTT Behavior and Properties

Figure 2 shows basic statistics of TUTTs for each year in ERA5. There is a remarkable long-term consistency in the number of tracked TUTTs per year (Fig. 2a). The median number of TUTTs per year is 8 with a standard deviation of just 2. Figure 2b shows the statistics of

TUTT longevity broken down by year. Longevity is more disperse than number and there is a weak increase of about 11 hours between 1979 and 2018 (~3% per decade). Given the possibility for this long-term trend to be influenced by changes in the observing network that provides input to the ERA5 reanalysis, we do not investigate it further here. Overall, the trends we observe are weaker than those of Douglas and Englehart (2007a) who show an increase in total inverted trough counts between 1976 and 2001 of about 14% per decade although it remains possible theirs was mostly driven by drought in the 1970s. A limitation of our statistics on TUTT lifetime is that we set an eastern boundary on the domain in which TUTTs are identified, which means some vorticity anomalies that originate east of our search domain are only counted as TUTTs after being advected into that domain (see Fig. S5a).

3.1 Genesis

To begin to investigate the physics of TUTTs, we examine the meteorology of North America before and during TUTT formation. As an example, we show 200 hPa PV (which is not used directly as a tracking variable in our application of TempestExtremes) and track center from our dataset for the TUTT previously described by Finch and Johnson (2010) and Newman and Johnson (2012) (#4 in Table 1). TempestExtremes identifies a TUTT beginning late on July 8^{th} which survives until July 14^{th}. In Figure 3, we show PV beginning on the 7^{th} at 12Z for meteorological context prior to TUTT genesis. All panels include the PV in colored contours and a red dashed line which marks the northernmost switch in the plotted domain from westerlies to easterlies at 200 hPa. Additionally, latter panels include a pink star marking the location of the TUTT center for the indicated day at 12Z. From July 7^{th} through the 9^{th}, a deep extratropical trough over the central US breaks (Haynes & McIntyre, 1987) and some of the high PV becomes embedded within the lower latitude easterlies. The TUTT center identified on July 9^{th} is clearly associated with anomalous PV over the Mississippi river and Gulf of Mexico. The TUTT center maintains its clear link to this PV source through (at least) July 12th. The TUTT moves westward slowly. Starting on the 9th, it becomes embedded in a region of weak upper-level easterlies. While we will show later that TUTTs are nearly round in a composite sense (Fig. 4), the PV associated with TUTT 4 is irregularly shaped and variable over the lifetime of the feature.

This kind of midlatitude-turned-subtropical PV feature has been discussed in detail in the context of events in South Asia by Ortega et al. (2017). They describe a "quasi-biweekly" process by which midlatitude Rossby waves break as they move off the east coast of Asia into the Pacific, a preferred region for Rossby wave breaking (Abatzoglou & Magnusdottir, 2006; Homeyer & Bowman, 2013). These events inject cyclonic energy into the subtropical easterlies and are hypothesized to eventually enhance precipitation in the Indian monsoon (Ortega et al., 2017). Potentially leading to a similar situation in the western hemisphere, summertime Rossby wave breaking and associated PV streamers are also common over North America and the western Atlantic (Homeyer & Bowman, 2013; Papin et al., 2020). Bosart et al. (2011) linked subsynoptic-scale PV disturbances to mesoscale convection in the NAM. Sierks et al. (2020) linked wave breaking directly to enhanced precipitation in the NAM, and Pytlak et al. (2005) noted westerly energy wrapping into the easterlies in association with TUTTs. To get a sense for how common this development sequence may be for TUTTs over North America, we have included an assessment of whether midlatitude wave breaking is associated with TUTT genesis for the disturbances listed in Table 1. Map sequences like that in Fig. 3 are included for each identified 2004 TUTT as Supporting Information. While we cannot say that TUTTs are *caused* by breaking, for three of the five NAME-year TUTTs, genesis is obviously *related* to midlatitude wave breaking near the latitude separating easterlies and westerlies. TUTT 7a/b (Fig. S3) and α

(Fig. S4) are similar in that there is wave breaking into the subtropics coincident with TUTT genesis, but in both cases, the breaking is well to the east of our search domain. For 7a/b and α, we deem wave breaking to be plausibly associated with TUTT genesis, but the direct link is not clear from the Figs. S3 and S4 alone. In all cases for the year 2004, TUTT centers are located south of the transition to easterlies despite frequently occurring at latitudes where westerlies are common. In most cases, including for TUTT 4 shown in Fig. 3, the meteorology of the CONUS is dominated by troughing on the east and west coasts with ridging (an enhanced monsoon ridge) two days prior to TUTT genesis. This pattern can be clearly seen in Fig. 3 for TUTT 4 as well as in a mean sense in the 200 hPa geopotential patterns two days prior to genesis (Fig. S5), and suggests that anticyclonic flow around the upper-level monsoon high advects vorticity anomalies into the NAM domain. Although the anomaly of the geopotential pattern prior to genesis is weak, it does suggest the upper-level pattern is amplified relative to climatology between the eastern Pacific and the peak of the monsoon ridge. Finally, while Ortega et al. (2017) observe a 10-20 day cycle in events in south Asia, mean and median TUTT genesis periods for events in the same year in our data are ~7 days and ~6 days.

3.2 Dynamics

Above, we largely examined the properties of *individual* TUTTs. But one of the benefits of tracking TUTTs (and one of our goals in so doing) is that we can easily examine their *composite* properties. Composites are constructed about the center of identified TUTTs (i.e. approximately about minima in 200 hPa stream function). We composite data from all times with an identified TUTT equally rather than compositing by per-TUTT means. This choice allows TUTT composites to be mechanistically linked as it retains relatable magnitudes among composites. But, it has the potential to weight the composite properties to particularly strong and/or long-lived events. Figure 4 shows the composite mean PV structure of TUTTs at 200 hPa and 500 hPa, giving a sense for the size and intensity of TUTTs. The composite TUTT reaches a peak intensity of ~3 PVU at 200 hPa and exhibits a slight southwest-to-northeast tilt. At 500 hPa, TUTTs only weakly influence the PV field. As their name would imply, Fig. 4 confirms TUTTs are largely upper tropospheric features; this might seem unsurprising given our choice to track 200 hPa streamfunction anomalies, but Boos et al. (2015) found peak PV at 500 hPa for disturbances identified by tracking 850 hPa relative vorticity anomalies in the South Asian monsoon. Figure 4 also shows the bulk shear of the composite wind field between two pairs of levels. The lower layer shear (850 hPa to 500 hPa) maximizes on the northwestern side of TUTTs whereas the upper layer shear (500 hPa to 200 hPa) maximizes on the southern side and minimizes near the center of the vortex. As indicated by the composites of vertical shear, rotational flow around the TUTT center extends radially outward to about 8° great circle distance, suggesting that any precipitation anomalies caused by this shear or by quasi-geostrophic uplift within the TUTT should be located within that radius (this will be discussed in detail in following subsections).

In the simplest sense, TUTT motion appears to be due to advection of the upper-level vortex by the horizontal wind. Figure 5 shows TUTT-mean horizontal wind at 500 hPa and 100 hPa. While these levels bracket that of the peak intensity of the rotational flow at 200 hPa, Fig. 5 clearly shows that easterlies dominate across much of the domain and especially near the TUTT center. Thus, TUTTs appear to be advected over the NAM region by the background flow from their source region east of the Rockies, though comparison of Fig. 1b to Fig. 5 suggests TUTTs move more slowly than the background wind above and below their center of peak vorticity.

Data in Fig. 5 is overlain on a map centered on the mean location of TUTT centers, for a sense of scale.

Next, we examine the vertical structure of TUTTs with composite vertical cross sections (Fig. 6). Figure 6a shows the composite mean vorticity structure of TUTTs averaged meridionally within 5 degrees latitude of the composite mean center. Figure 6b shows a similar zonal mean latitude-height composite. It should be noted that in the height profiles we present (Fig. 6, 7c, and 8), some of the input data to our composites from some TUTT times and locations may be below ground and extrapolated in the reanalysis. The mean surface pressure across all TUTTs at the TUTT center is 950 hPa. Consequently, the lowest levels in height profiles should be interpreted cautiously. The intensity of TUTT vorticity peaks at 200 hPa (which is also the level at which we identify cyclonic features from the stream function) and is weak below 500hPa, if it exists at all there. The composite TUTT is embedded within a region of anticyclonic circulation, consistent with the view that TUTTs are isolated cyclonic circulations generally moving westward in a deep monsoon anticyclone.

To create meaningful composites of some physical quantities, we added a new capability to TempestExtremes. The climatological patterns of vertical velocity and precipitation are highly dependent on local geography over North America and on the general circulation of the atmosphere across the tropics. For example, higher rainfall amounts occur climatologically during July and August near the southern edge of our search domain over ocean, and locally over high terrain. To prevent these climatological background signals from imprinting themselves on composites of TUTT properties, we construct composites of anomaly fields. The anomaly is here defined as the instantaneous field measure minus the long-term background state, which is composed of the first four intra-annual Fourier modes of the daily climatological mean. The first four modes are kept because they recreate the NAM seasonal cycle of precipitation well but eliminate large short-term fluctuations that exist in the mean calculated from 16 years of TRMM data (see §4 below).

Figure 6a includes the composite of meridional mean anomalous vertical pressure velocity. In the upper troposphere below 200 hPa, TUTTs exhibit a zonal dipole of ascent, with subsidence to the west and ascent to the east of the circulation center. In the middle to lower troposphere, weak subsidence occurs at the circulation center while modest ascent peaks about 1000 km to the east. This structure is in keeping with TUTTs studied in the north Pacific (Kelley & Mock, 1982; Whitfield & Lyons, 1992). TUTTs exist in a region in which the climatological shear of the zonal wind is eastward below 200hPa and westward above. Therefore, the anomalous vertical velocity expected in QG flow around a vortex changes sign at 200 hPa, consistent with the quadrupole in anomalous vertical velocity seen in the upper troposphere in Fig. 6a. Along the meridional cross section (Fig. 6b), zonal mean vertical velocity is strongly upward to the south of the vortex center and downward below the center and to the north (note the change in color scale between Figs. 6a and 6b). The strongest upward motion is located in the lower troposphere about 15° of latitude south of the TUTT center, and is likely associated with the East Pacific ITCZ (compare with the average TUTT position shown in Fig. 5, which would place that peak ascent south of Central America near 10°N). Taken together, these figures imply a region of strong anomalous upward motion near the climatological ITCZ, with the periphery of that anomalous ascent extending into the southern part of TUTTs and wrapping around to the east as one ascends from the surface to 200hPa.

We have also examined the dynamics responsible for the vertical motion distribution shown in Figure 6 using the traditional form of the QG ω equation. Specifically, we inverted the adiabatic terms representing differential geostrophic absolute vorticity advection and the horizontal Laplacian of horizontal geostrophic thickness advection, applied to the composite wind and thermodynamic fields. To faithfully compare composite anomalous ω to that derived from QG, Fig. 7a shows anomalous ω at 250 hPa minus the domain mean anomalous ω. This is a necessary complication given the composite nature of our input. The pattern thus produced shows primary uplift in the southeast quadrant of the TUTT and subsidence immediately to the northwest, with maxima within a few hundred kilometers of the TUTT center. Figure 7b shows the same map derived from inverting the QG omega equation. The pattern and magnitude of the pressure velocity are similar. This implies that the upper-level ascent and descent in the vicinity of a TUTT center is largely the result of dry adiabatic processes rather than some interaction with moist convection, a notable finding given the great importance of diabatic effects for ascent in lower-tropospheric vortices in some monsoon regions (e.g. Murthy and Boos 2019). Figure 7c shows vertical profiles of pressure velocity. The solid lines show profiles of pressure velocity for a square region 5° on a side located to the southeast of the composite center minus the respective domain mean (i.e. what is shown in the previous panels). The dashed lines show the respective domain mean profiles. There is a deep layer of uplift to the southeast of the TUTT center that peaks near 250 hPa. This layer lies between two layers of descent. The QG analysis does a good job approximating the shape and magnitude of the composite anomalous ω in these layers. This implies that the upper-level dynamics of TUTTs can be reasonably well understood with QG kinematics. However, the QG inversion fails to recreate the anomalous descent seen between the surface and 500 hPa in the composite; diabatic processes, such as friction with the high topography in the NAM region, may be important there.

The domain mean composite anomalous ω (dashed red line in Fig. 7c) is dominated by the strong ascent 1000-1500 km south of the TUTT center (Fig. 6b). This raises an important question about TUTTs. Do TUTTs somehow cause anomalous ascent in the East Pacific ITCZ, or do their genesis, propagation, and sustenance occur in response to the intensification of the ITCZ? Alternatively, are the ITCZ and TUTTs both modulated by some larger-scale event, such as the wave breaking portrayed in Fig. 3? Answering this question is beyond the scope of this investigation.

3.3 Moisture

Figure 8 shows composite cross sections of the relative humidity of TUTTs. The west-to-east cross section in Fig. 8a shows the lowest values of boundary layer humidity lie on the western side of the TUTT; boundary layer-to-midlevel humidity is lesser there, as is humidity within TUTT cores above 500 hPa. In the wake of TUTTs to the east, the composite shows higher upper-level humidity than to the west. The north-to-south cross section exhibits a meridional gradient (consistent with climatology) at most levels. Together, these suggest TUTTs are the moistest to their south and east but that they are not particularly moist systems. In their cores, they are, in fact, rather dry for systems which have been claimed to cause precipitation enhancement. The water vapor scale height within the TUTT core is about 50 m lower than outside the TUTT core (not shown directly). So, TUTT cores are slightly less moist and their moisture is concentrated at lower altitudes. This combination would tend to suppress growth of deep convection within TUTT cores relative to TUTT edges.

Figure 9 shows the composite mean anomalous 850 hPa wind overlain on the composite mean 850 hPa water vapor mixing ratio. This figure is designed to illustrate the association of TUTTs with anomalous horizontal moisture advection and low-level convergence. There is a clear enhancement of near-surface anticyclonic circulation to the northeast of the TUTT center. Given the composite center location is in central Mexico, this might be related to a strengthening of the North American low-level jet, though it is unclear why this would be associated with TUTTs. There is an anomalous convergence line at about -10° likely associated with a shift or strengthening of the ITCZ. Figure 9 shows there is dry advection to the northwest of TUTTs and within the western half of the TUTT itself; mixing ratios are also larger to the east of the TUTT than to the west, likely due to the TUTT's mean location just west of the Gulf of Mexico (e.g. Fig. 5). *A priori*, it was not obvious whether TUTTs would affect moisture advection significantly since TUTTs are inherently upper tropospheric features with low boundary layer relative humidity (Fig. 8). TUTT cores mostly experience near neutral low-level moisture advection, and there is no indication that TUTTs produce any cyclonic stirring across the climatological mean moisture gradient.

4. TUTTs and Precipitation

As discussed in the Introduction, previous studies have suggested that TUTTs may be felt most strongly in the arid NAM region through their impact on precipitation. Figure 10 shows the TUTT-mean anomalous TRMM precipitation rate where, as above, anomalies are calculated as deviations from a daily mean which retains the first four Fourier modes calculated from 1998 to 2013. We use 3-hourly TRMM precipitation estimates at 0.25° (3B42 version 7)(Huffman et al., 2007). Figure 10 has been masked for statistical significance by comparing the statistics of the distribution of rainfall rates for TUTT cases against a climatology. Filled contours show the mean anomalous precipitation rate for TUTT rainfall distributions which pass a two-sided *t*-test at the 90% level against the climatology. The climatology is constructed by randomizing the year but not the date of TUTTs and re-compositing. In this way, we ensure that the climatology contains the same number of samples from the same geographic locations with the same potential for autoregression in the data as the TUTT dataset. Approximately half of all points are deemed statistically significant by this strict test.

The most coherent signal to emerge from the data is that of a decrease in the magnitude of precipitation within the TUTT and to its north and northeast; the peak reduction in rainfall is centered on the west side of the TUTT, in the region where the anomalous low-level winds would be expected advection in dry air, given the total moisture gradient (Fig. 9). There are also several small contiguous regions of precipitation enhancement east, south, and west of the TUTT center.

The decrease in precipitation within the TUTT core is associated with the subsidence (Fig. 6) that occurs at most levels north of the TUTT center and at the mid- to low-levels in the TUTT center. It is unclear whether the subsidence anomaly is causing the precipitation anomaly, or vice-versa, a common issue in low-latitude atmospheric dynamics. Moreover, we identify no clear cause of either of these anomalies in the TUTT center. While some low-level positive moisture advection occurs north of TUTT cores (Fig. 9), it does not effect an enhancement of precipitation. One way to untangle this ambiguity in the future would be to examine TUTTs in large-domain, convection-permitting simulations (Luong et al., 2017; Prein et al., 2015).

There are, however, several regions of precipitation enhancement to the south of TUTTs. These contiguous regions of precipitation enhancement occur in a region of anomalous ascent (in a composite sense; Fig. 6), higher humidity (Fig. 8), neutral to anticyclonic rotation (Fig. 6), and largely in regions of weak upper tropospheric shear (Fig. 4d). They also seem to occur in regions of anomalous 850 hPa convergence but not necessarily in regions of positive moisture advection (Fig. 9). We will note two possible explanations for precipitation enhancement. First, because the composite central location of TUTTs lies over central Mexico, the southern and eastern sides of TUTTs are coincident with steep topography and on-shore flow. This combination may act to enhance precipitation locally through upslope flow or frictional convergence, and the on-shore flow may be associated with the larger-scale easterlies within which the TUTT is embedded rather than the rotational flow of the TUTT itself. Second, the anomalous convergence well to the south of TUTTs may correspond to an enhanced or displaced ITCZ. The ITCZ modulation might be caused by the same wave-breaking activity that generated the TUTT, but how and why the ITCZ and TUTTs interact is unknown.

It is possible that TUTTs influence precipitation in geographically specific ways that vary along their full tracks. For example, case studies of TUTTs (e.g. Pytlak et al. 2005; Newman and Johnson 2012; Finch and Johnson 2010) often illustrate the scattered nature of convection associated with TUTTs in northwestern Mexico. This is in keeping with our synthesis which shows mixed impacts and only that the composite *mean* precipitation rate is lower within TUTT centers, not that high rain rates never occur in TUTTs. The upper-tropospheric nature of TUTTs seems to limit their ability to directly enhance precipitation; they produce ascent over a deep layer of the upper troposphere in their southeastern quadrant, with that ascent well-represented by quasi-geostrophic solutions unmodified by diabatic heating. This would have much in common with the vorticity anomalies in the Tibetan Plateau anticyclone, which Hsu and Plumb (2000) found were confined to the upper troposphere. Finally, we will also note that TRMM surface precipitation may be biased across high desert landscapes like those of the NAM region, so our results should be interpreted accordingly (Huffman et al., 2007).

One of the conclusions from the NAME was that TUTTs act to enhance precipitation on their southeastern side *and* on their northwestern side (Finch & Johnson, 2010; Newman &

Johnson, 2012; Pytlak et al., 2005). Figure 10 does contain positive precipitation anomalies northwest of the TUTT center, but these did not pass the screen for statistical significance. Figure 11 shows the 95th percentile of anomalous TRMM precipitation calculated for a 5° wide band starting in the southeastern corner of our composite domain and proceeding past the TUTT center to the northwestern corner. The black line shows the result for all years. The figure implies the same result as above; precipitation is enhanced southeast of TUTTs, with the most extreme rainfall occurring more than 500 km southeast of the TUTT center. Underlain on Fig. 11 are similarly constructed composites for each TRMM year. These are largely similar to each other and the mean except for the dashed burgundy line which shows an enhancement of precipitation of about 1 mm hr^{-1} on the northwestern side of TUTTs during the NAME year (2004). We included this figure to further our assertion that our automated tracking of TUTTs is consistent with those done by hand, but it also raises the interesting question (or perhaps specter) of whether TUTTs were somehow characteristically different during the NAME year. Does the assimilation of NAME data from an otherwise sparsely observed region of North America in the ERA5 reanalysis impact that dataset's upper-tropospheric flow field, allowing ERA5 to better represent TUTTs in 2004 than in all other years? We will leave this question unanswered but provide one thought. The proposed mechanism for the enhancement of precipitation in the northwest quadrant of TUTT 4 in Newman and Johnson (2012) relies explicitly on topographically aided lifting. TUTTs may have tracked preferentially in 2004 such that small scale topographic features could help generate lift at the leading edge of TUTTs. This is speculative, as we notice nothing extraordinary about their tracks at the large scale (not shown). Finally, we will also note that we reconstructed Fig. 11 using ERA5 precipitation to the same result (not shown).

5. Summary and Conclusions

The goal of this paper was to identify and track TUTTs in time and space in a high-resolution, high-quality dataset and to better understand the relationship of TUTTs with precipitation. We used TempestExtremes to track upper-level circulation centers in the ERA5 reanalysis from 1979 to 2018. Our criteria resulted in 340 long-lived TUTTs over the NAM region, which proved enough to paint a composite picture of these features.

We found that TUTTs exist primarily as upper-tropospheric features that, based on case studies, seem to originate from midlatitude wave breaking to the east of the NAM. TUTTs exhibit high-PV, dry air and travel westward within the mean easterly upper-level flow. Our most notable finding is that precipitation is not systematically enhanced within the main rotational flow of the TUTT. Specifically, we found no detectable increase in precipitation on the western or northwestern sides of TUTTs in the composite mean. This result contrasts with previous arguments, which relied heavily on case studies during the NAME year, that precipitation is enhanced on the western side of TUTTs due to modulations of CAPE and layer shear that enhance MCS formation (e.g. Finch and Johnson 2010, Newman and Johnson 2012). Our analysis confirms that precipitation was enhanced northwest of TUTTs during the NAME year (Fig. 11), but that year was an outlier in the combined TRMM and ERA5 datasets on which our analysis was based. This could indicate that TUTT tracks were unusual in the NAME year, consistent with the anomalously short monsoon season and poorly developed subtropical high during that year (e.g. Douglas and Englehart, 2007), or that the ERA5 reanalysis has deficiencies in its representation of TUTTs outside the NAME year. Because our conclusions regarding precipitation contrast starkly with those of previous studies, we again want to point out that TRMM 3B42 is an imperfect tool for assessing surface precipitation over the high desert but that its use in this study was necessitated by our need for a long data record. Future studies might be better served by employing a more modern tool (e.g. the GPM period of IMERG or GSMaP) when any has a long enough, homogenous data record. We also found that the quasi-geostrophic ascent in the southeastern quadrant of the TUTT does not enhance precipitation and seems to be confined to the upper troposphere. Although other studies previously examined QG ascent in transient disturbances in the NAM region (e.g. Seastrand et al. 2015), our results provide the first analysis of QG vertical motion in a large ensemble of upper-tropospheric vorticity anomalies.

Our study has focused on the mean properties of TUTTs at the expense of deeper understanding of individual events within our dataset. An obvious omission, then, is that we have not utilized the time-space evolution data to its fullest extent. We see two opportunities in this regard for future studies. 1) We examined Rossby Wave breaking and TUTT genesis for NAME year TUTTs only. Automating that examination by pairing our data to a wave breaking database (e.g. Abatzoglou & Magnusdottir, 2006) would show statistically how frequently TUTTs are associated with summer-time wave breaking and *vice versa*. 2) Many previous investigations of TUTTs have focused on their (potentially) transient interaction with other meteorological or topographic features which may significantly, though temporarily, alter their impacts. Given the episodic nature of precipitation, it's possible that our composite view misses some interesting TUTT behavior. Employing evolutionary prototype methods (e.g. Igel 2018) might help to categorize and identify frequent development patterns of precipitation throughout the lifetime of TUTTs that are difficult to recognize from composites.

6. Appendix

The TempestExtremes v2.0 feature identification command is: `DetectNodes --in_data_list Inputfile --out Outputfile --searchbymin` `“streamfunction” --minlat 15 --maxlat 40 --minlon -120 --maxlon -90 –noclosedcontourcmd “Z,325.,4.0,1.0” --mergedist 5.0` . The command to stitch identified features in time is: `StitchNodes --in Outputfile --out StitchOutputfile --maxgap 1 --minlength 67 --range 5.0`.

Acknowledgements

This material is based upon work supported by the U.S. Department of Energy, Office of Science, Office of Biological and Environmental Research, Climate and Environmental Sciences Division, Regional and Global Model Analysis Program, under Award DE-SC0019367. It used resources of the National Energy Research Scientific Computing Center (NERSC), which is a DOE Office of Science User Facility. Special thanks to M. Diaz for help and D. Shaevitz for providing the QG ω inversion code.

Data Availability Statement

ERA5 data are available at https://cds.climate.copernicus.eu/#!/search?text=ERA5&type=dataset. TRMM data are available https://gpm.nasa.gov/data-access/downloads/trmm. The TempestExtremes source code is available at https://github.com/ClimateGlobalChange/tempestextremes. The new TUTT dataset is available at https://doi.org/10.25338/B8VS7T .

References

Abatzoglou, J. T., & Magnusdottir, G. (2006). Planetary Wave Breaking and Nonlinear Reflection: Seasonal Cycle and Interannual Variability. *Journal of Climate*, *19*(23), 6139–6152. https://doi.org/10.1175/JCLI3968.1

Adams, D. K., & Comrie, A. C. (1997). The North American Monsoon. *Bulletin of the American Meteorological Society*, *78*(10), 2197–2213. https://doi.org/10.1175/1520-0477(1997)078<2197:TNAM>2.0.CO;2

Bieda, S. W., Castro, C. L., Mullen, S. L., Comrie, A. C., & Pytlak, E. (2009). The relationship of transient upper-level troughs to variability of the North American monsoon system. *Journal of Climate*, *22*(15), 4213–4227. https://doi.org/10.1175/2009JCLI2487.1

Boos, W. R., Hurley, J. V., & Murthy, V. S. (2015). Adiabatic westward drift of Indian monsoon depressions. *Quarterly Journal of the Royal Meteorological Society*, *141*(689), 1035–1048. https://doi.org/10.1002/qj.2454

Bosart, L., Melino, T. J., Sukup, S. R., Pytlak, E. S., E., M. J., Weiss, S. J., et al. (2011). Potential vorticity disturbances as a trigger of southwest U.S. severe weather. In *24th Conference on Weather and Forecasting/20th Conference on Numerical Weather Prediction*.

Douglas, A. V., & Englehart, P. J. (2007a). A climatological Perspective of transient synopic features during NAME 2004. *Journal of Climate*, *20*(9), 1947–1954. https://doi.org/10.1175/JCLI4095.1

Douglas, A. V., & Englehart, P. J. (2007b). A Climatological Perspective of Transient Synoptic

Features during NAME 2004. *Journal of Climate*, *20*(9), 1947–1954. https://doi.org/10.1175/JCLI4095.1

Finch, Z. O., & Johnson, R. H. (2010). Observational analysis of an upper-level inverted trough during the 2004 north american monsoon experiment. *Monthly Weather Review*, *138*(9), 3540–3555. https://doi.org/10.1175/2010MWR3369.1

Haynes, P. H., & McIntyre, M. E. (1987). On the Representation of Rossby Wave Critical Layers and Wave Breaking in Zonally Truncated Models. *Journal of the Atmospheric Sciences*, *44*(17), 2359–2382. https://doi.org/10.1175/1520-0469(1987)044<2359:OTRORW>2.0.CO;2

Hersbach, H., Bell, B., Berrisford, P., Hirahara, S., Horányi, A., Muñoz-Sabater, J., et al. (2020). The ERA5 Global Reanalysis. *Quarterly Journal of the Royal Meteorological Society*, qj.3803. https://doi.org/10.1002/qj.3803

Higgins, W., Ahijevych, D., Amador, J., Barros, A., Berbery, E. H., Caetano, E., et al. (2006). The NAME 2004 Field Campaign and Modeling Strategy. *Bulletin of the American Meteorological Society*, *87*(1), 79–94. https://doi.org/10.1175/BAMS-87-1-79

Homeyer, C. R., & Bowman, K. P. (2013). Rossby Wave Breaking and Transport between the Tropics and Extratropics above the Subtropical Jet. *Journal of the Atmospheric Sciences*, *70*(2), 607–626. https://doi.org/10.1175/JAS-D-12-0198.1

Hsu, C. J., & Plumb, R. A. (2000). Nonaxisymmetric Thermally Driven Circulations and Upper-Tropospheric Monsoon Dynamics. *Journal of the Atmospheric Sciences*, *57*(9), 1255–1276. https://doi.org/10.1175/1520-0469(2000)057<1255:NTDCAU>2.0.CO;2

Huffman, G. J., Bolvin, D. T., Nelkin, E. J., Wolff, D. B., Adler, R. F., Gu, G., et al. (2007). The TRMM Multisatellite Precipitation Analysis (TMPA): Quasi-Global, Multiyear, Combined-Sensor Precipitation Estimates at Fine Scales. *Journal of Hydrometeorology*, *8*(1), 38–55. https://doi.org/10.1175/JHM560.1

Igel, M. R. (2018). Lagrangian Cloud Tracking and the Precipitation-Column Humidity Relationship. *Atmosphere*, *9*, 289. https://doi.org/10.3390/atmos9080289

Johnson, R. H., Ciesielski, P. E., McNoldy, B. D., Rogers, P. J., & Taft, R. K. (2007). Multiscale Variability of the Flow during the North American Monsoon Experiment. *Journal of Climate*, *20*(9), 1628–1648. https://doi.org/10.1175/JCLI4087.1

Kalnay, E., Kanamitsu, M., Kistler, R., Collins, W., Deaven, D., Gandin, L., et al. (1996). The NCEP/NCAR 40-Year Reanalysis Project. *Bulletin of the American Meteorological Society*, *77*(3), 437–471. https://doi.org/10.1175/1520-0477(1996)077<0437:TNYRP>2.0.CO;2

Kelley, W. E., & Mock, D. R. (1982). A diagnostic study of upper tropospheric cold lows over the western North Pacific (Guam, Midway, Johnston, Wake). *Monthly Weather Review*. https://doi.org/10.1175/1520-0493(1982)110<0471:ADSOUT>2.0.CO;2

Kelly, W. E., & Mock, D. R. (1982). A Diagnostic Study of Upper Tropospheric Cold Lows Over the Western North Pacific. *Monthly Weather Review*, *110*(6), 471–480. https://doi.org/10.1175/1520-0493(1982)110<0471:ADSOUT>2.0.CO;2

Krishnamurti, T. N., & Bhalme, H. N. (1976). Oscillations of a Monsoon System. Part I. Observational Aspects. *Journal of the Atmospheric Sciences*, *33*(10), 1937–1954. https://doi.org/10.1175/1520-0469(1976)033<1937:OOAMSP>2.0.CO;2

Lahmers, T. M., Castro, C. L., Adams, D. K., Serra, Y. L., Brost, J. J., & Luong, T. (2016). Long-term changes in the climatology of transient inverted troughs over the North American monsoon region and their effects on precipitation. *Journal of Climate*, *29*(17), 6037–6064. https://doi.org/10.1175/JCLI-D-15-0726.1

Luong, T. M., Castro, C. L., Chang, H. I., Lahmers, T., Adams, D. K., & Ochoa-Moya, C. A. (2017). The more extreme nature of North American Monsoon precipitation in the Southwestern United States as revealed by a historical climatology of simulated severe weather events. *Journal of Applied Meteorology and Climatology*, *56*(9), 2509–2529. https://doi.org/10.1175/JAMC-D-16-0358.1

Murthy, V. S., & Boos, W. R. (2019). Quasigeostrophic Controls on Precipitating Ascent in Monsoon Depressions. *Journal of the Atmospheric Sciences*, *77*(4), 1213–1232. https://doi.org/10.1175/JAS-D-19-0202.1

Newman, A., & Johnson, R. H. (2012). Mechanisms for precipitation enhancement in a North American Monsoon upper-tropospheric trough. *Journal of the Atmospheric Sciences*, *69*(6), 1775–1792. https://doi.org/10.1175/JAS-D-11-0223.1

Ortega, S., Webster, P. J., Toma, V., & Chang, H. R. (2017). Quasi-biweekly oscillations of the South Asian monsoon and its co-evolution in the upper and lower troposphere. *Climate Dynamics*, *49*(9–10), 3159–3174. https://doi.org/10.1007/s00382-016-3503-y

Papin, P. P., Bosart, L. F., & Torn, R. D. (2020). A Feature Based Approach to Classifying Summertime Potential Vorticity Streamers Linked to RossbyWave Breaking in the North Atlantic Basin. *Journal of Climate*, 5953–5969. https://doi.org/10.1175/jcli-d-19-0812.1

Prein, A. F., Langhans, W., Fosser, G., Ferrone, A., Ban, N., Goergen, K., et al. (2015). A review on regional convection-permitting climate modeling: Demonstrations, prospects, and challenges. *Reviews of Geophysics*, *53*(2), 323–361. https://doi.org/10.1002/2014RG000475

Pytlak, E., Goering, M., & Bennett, A. (2005). Upper tropospheric troughs and their interaction with the North American Monsoon. *85th AMS Annual Meeting, American Meteorological Society - Combined Preprints*, (1992), 281–285.

Rogers, P. J., & Johnson, R. H. (2007). Analysis of the 13–14 July Gulf Surge Event during the 2004 North American Monsoon Experiment. *Monthly Weather Review*, *135*(9), 3098–3117. https://doi.org/10.1175/MWR3450.1

Seastrand, S., Serra, Y., Castro, C., & Ritchie, E. (2015). The dominant synoptic-scale modes of North American monsoon precipitation. *International Journal of Climatology*, *35*(8), 2019–2032. https://doi.org/10.1002/joc.4104

Sierks, M. D., Kalansky, J., Cannon, F., & Ralph, F. M. (2020). Characteristics, origins, and impacts of summertime extreme precipitation in the Lake Mead watershed. *Journal of Climate*, *33*(7), 2663–2680. https://doi.org/10.1175/JCLI-D-19-0387.1

Ullrich, P. A., & Zarzycki, C. M. (2017). TempestExtremes: A framework for scale-insensitive pointwise feature tracking on unstructured grids. *Geoscientific Model Development*, *10*(3), 1069–1090. https://doi.org/10.5194/gmd-10-1069-2017

Ullrich, P. A., Zarzycki, C. M., McClenny, E. E., Pinheiro, M. C., Stanfield, A. M., & Reed, K. A. (2021). TempestExtremes v2.1: A Community Framework for Feature Detection, Tracking and Analysis in Large Datasets. *Geoscientific Model Development Discussion*. https://doi.org/10.5194/gmd-2020-303

Whitfield, M. B., & Lyons, S. W. (1992). An Upper-Tropospheric Low over Texas during Summer. *Weather and Forecasting*, *7*(1), 89–106. https://doi.org/10.1175/1520-0434(1992)007<0089:AUTLOT>2.0.CO;2

Zarzycki, C. M., & Ullrich, P. A. (2017). Assessing sensitivities in algorithmic detection of tropical cyclones in climate data. *Geophysical Research Letters*, *44*(2), 1141–1149. https://doi.org/10.1002/2016GL071606

Tables

Table 1: Comparison TUTTs identified with Tempest Extremes and subjectively in Pytlak et al. (2005) and Sierks et al. (2020). For NAME year storms, a subjective assessment of whether the identified TUTT is generated by midlatitude wave breaking (as determined from Fig. 3 and Supporting figures) is included.

TUTT	Pytlak et al.	Tempest Extremes (Breaking?)	Permissive 0.75/1.75
3	7/5-7/10	7/3-7/6 (yes)	✓/✓
4	7/8-7/13	7/8-7/14 (yes)	✓/✓
5	7/15-7/18		✓/7/17-7/18
6	7/20-7/25	7/20-7/24 (yes)	✓/3 TUTTs
7a/b	7/29-8/2	7/29-8/1 (maybe)	✓/7/29-8/1
8	8/2-8/4		✓/x
9	8/7-8/10		✓/x
10	8/7-8/12		✓/x
α & Others		TUTT α: 7/24-7/27 (well to the east)	23/5

Inverted Trough/TUTT	Sierks et al	Tempest Extremes
A	8/24/1982	8/24-8/27
B	7/25/1983	7/22-7/25
C	7/22/1986	7/19-7/22
D	7/23/1998	7/20-7/27
E	7/9/1999	
F	8/30/2000	
G	7/27/2013	7/26-8/3
H	8/4/2014	

Figures

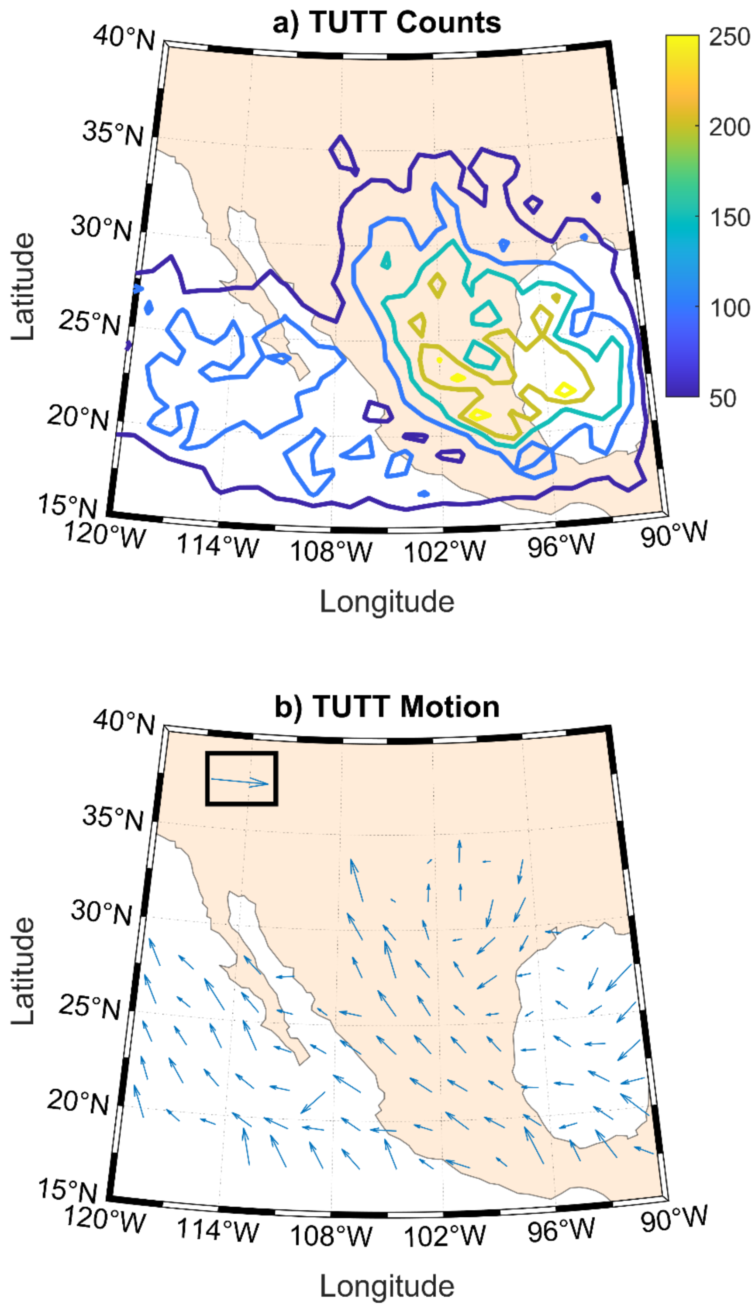
a) TUTT Counts
40°N
35°N
30°N
25°N
20°N
15°N
120°W
114°W
108°W
102°W
96°W
90°W
Latitude
Longitude
250
200
150
100
50
b) TUTT Motion
40°N
35°N
30°N
25°N
20°N
15°N
120°W
114°W
108°W
102°W
96°W
90°W
Latitude
Longitude

Figure 1: a) Total number of TUTT-center counts in 0.25° grid boxes. b) Mean TUTT-center velocity vectors in 0.50° grid boxes for such boxes with at least 50 TUTT centers. The scale of the arrow inside the black box is 5 m s^{-1}.

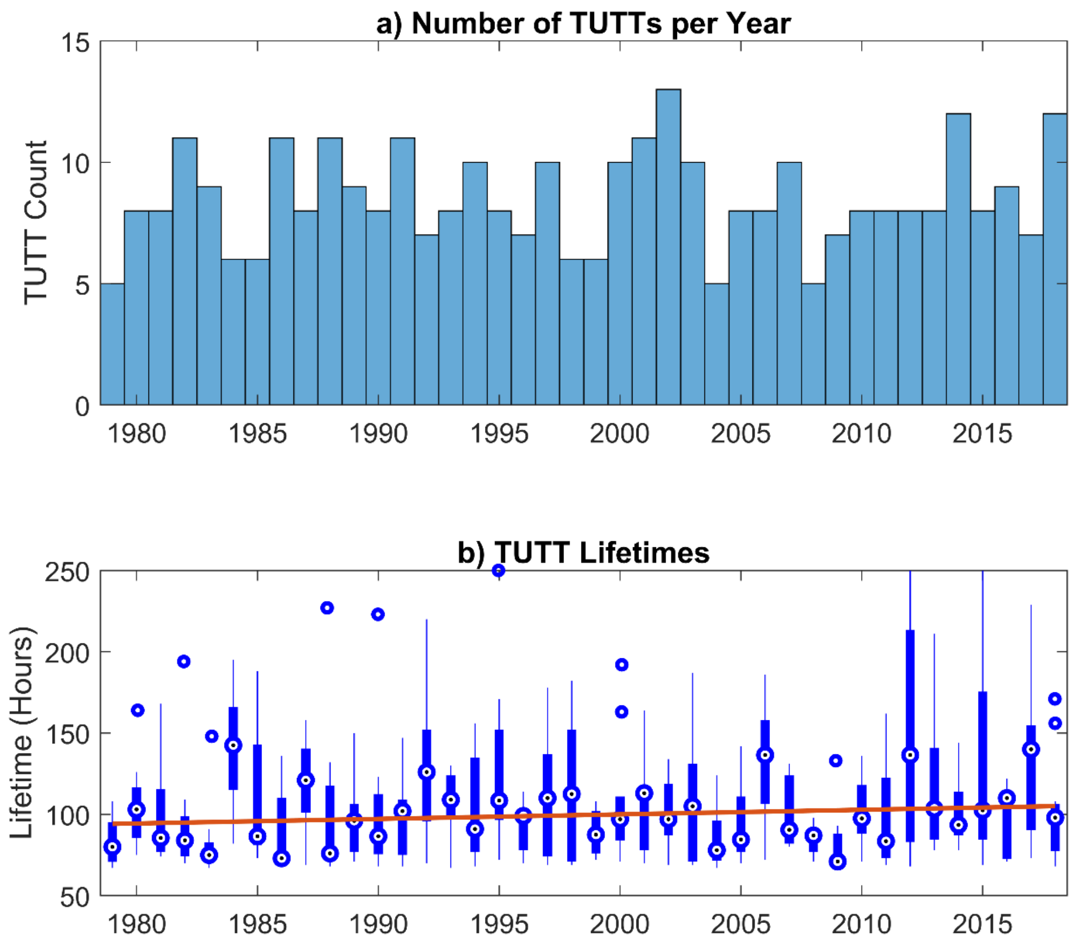

Figure 2: a) A bar plot of TUTT counts per year. b) Box and whisker plots of TUTT lifetimes per year. The red line is a best fit to the data of TUTT lifetimes to the year.

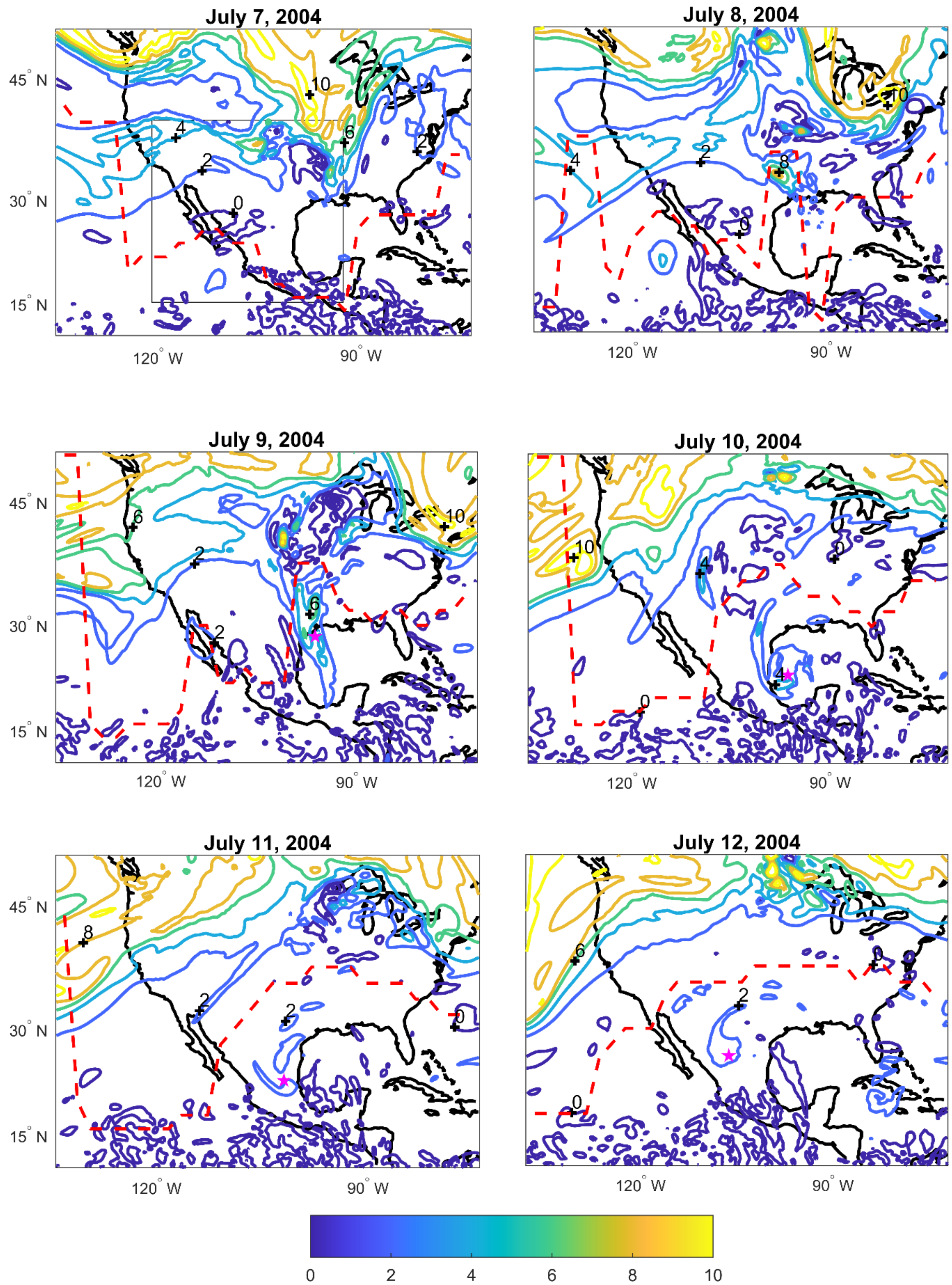

July 7, 2004
July 8, 2004
July 9, 2004
July 10, 2004
July 11, 2004
July 12, 2004
45° N
30° N
15° N
120° W
90° W
0
2
4
6
8
10

671

Figure 3: Maps of PV (color contours every 2 PVU with zero and negative values dark blue). PV contours are labeled intermittently near points of interest in figures for convenience. The red dashed line indicates the northernmost switch in the plotted domain from westerlies to easterlies. The pink star indicates the location of a TempestExtremes identified TUTT center. The black box included on July 7th marks the TUTT search domain.

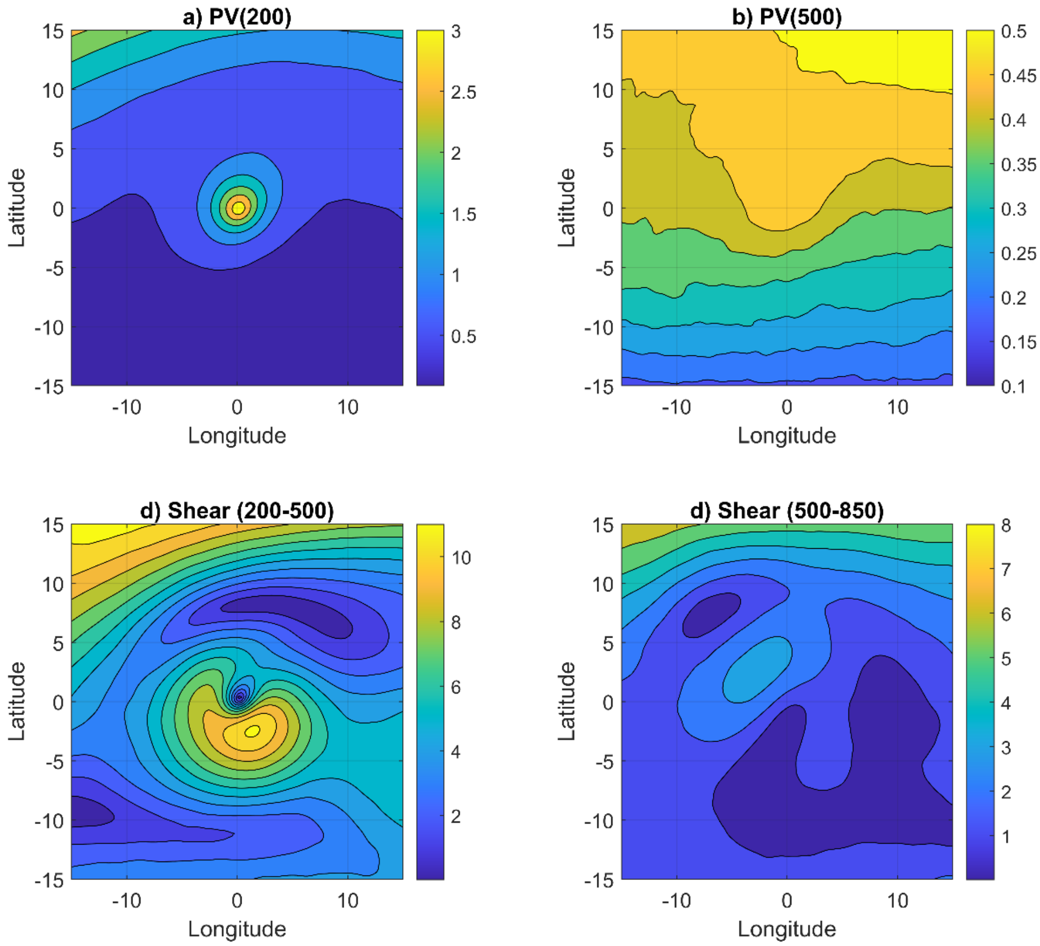

Figure 4: The top row shows composite mean PV at a) 200 hPa with contours spaced ever 0.5 PVU and b) at 500 hPa spaced every 0.05 PVU. The bottom row shows the magnitude of the vertical shear of the composite mean horizontal wind with contours spaced every 1 m s^{-1} between c) 200 hPa and 500 hPa and d) 500 hPa and 850 hPa.

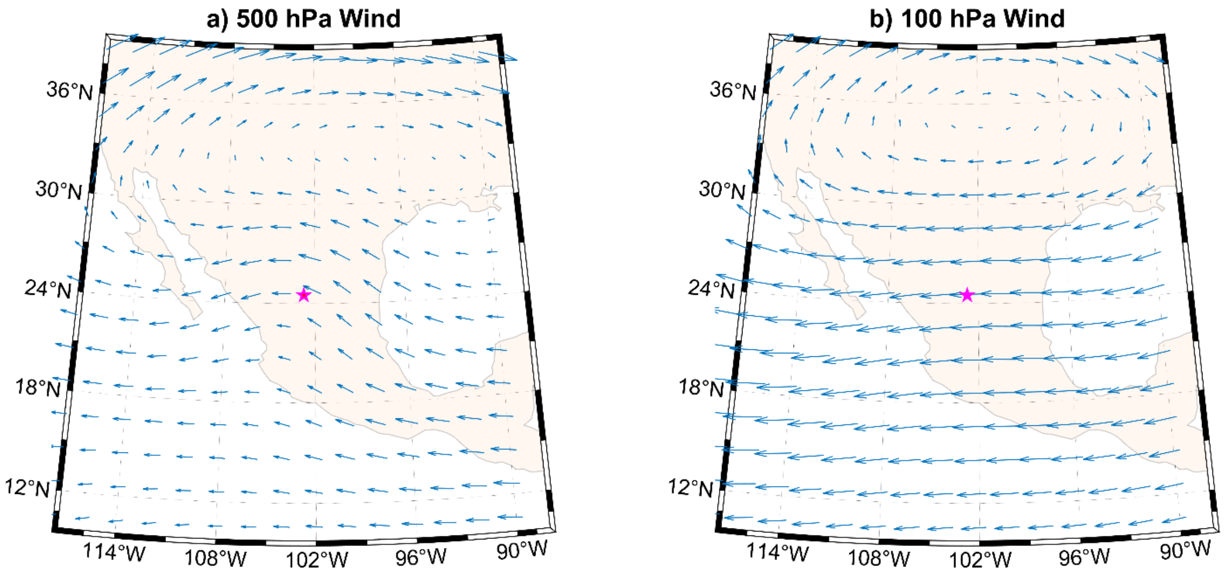

Figure 5: Wind vectors for the mean a) 500 hPa and b) 100 hPa flow. Composite mean flow is projected on a map centered on the mean TUTT center location for context which is marked with a red star. Wind vectors are plotted every 2°. The maximum magnitude of a wind barb in both a) and in b) is 10 m s^{-1}.

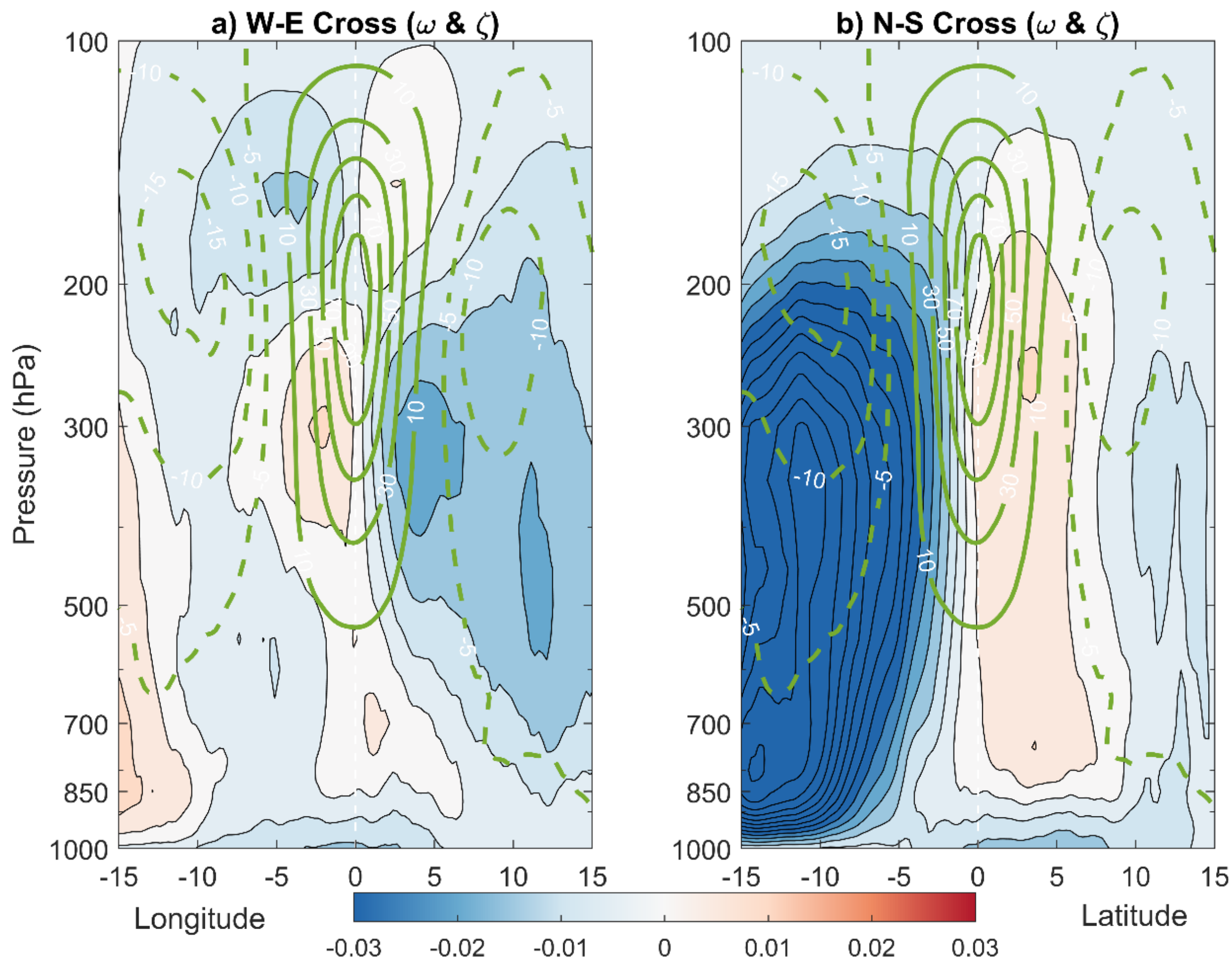

Figure 6: Composite mean cross sections of anomalous pressure velocity in colored shading and relative vorticity in green contours with white labels. a) A zonal cross section averaged within 5° latitude of the composite center. b) A meridional cross section averaged within 5° longitude of the composite center.

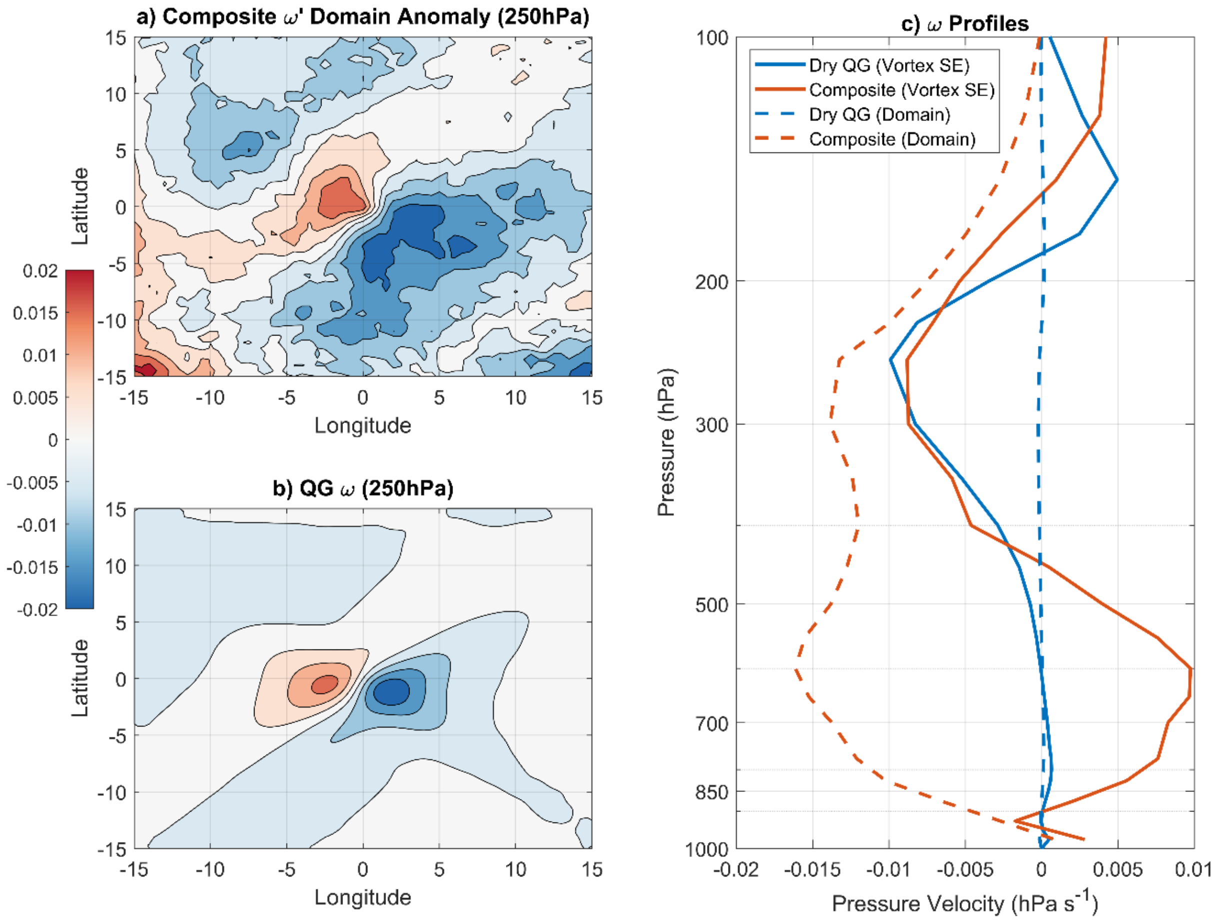

Figure 7: Comparisons between the anomaly of composite ω and that derived from the QG inversion. a) Map of the anomaly of composite ω at 250 hPa. b) Map of inverted QG ω. c) Vertical profiles of both ω quantities for a 5° square to the southeast of the vortex composite point and for the whole domain. “Dry QG” implies that we do not invert the diabatic term.

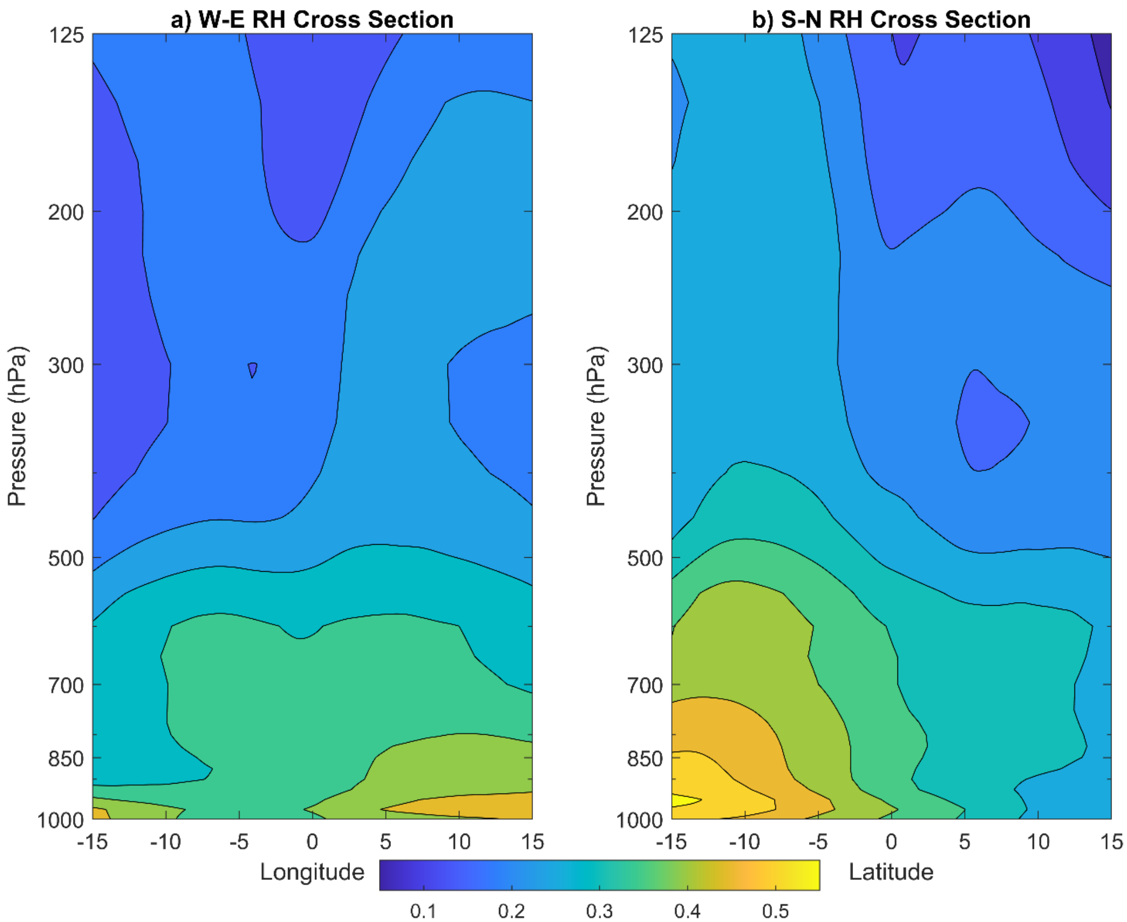

Figure 8: Like Fig. 6 except for relative humidity (not anomalous).

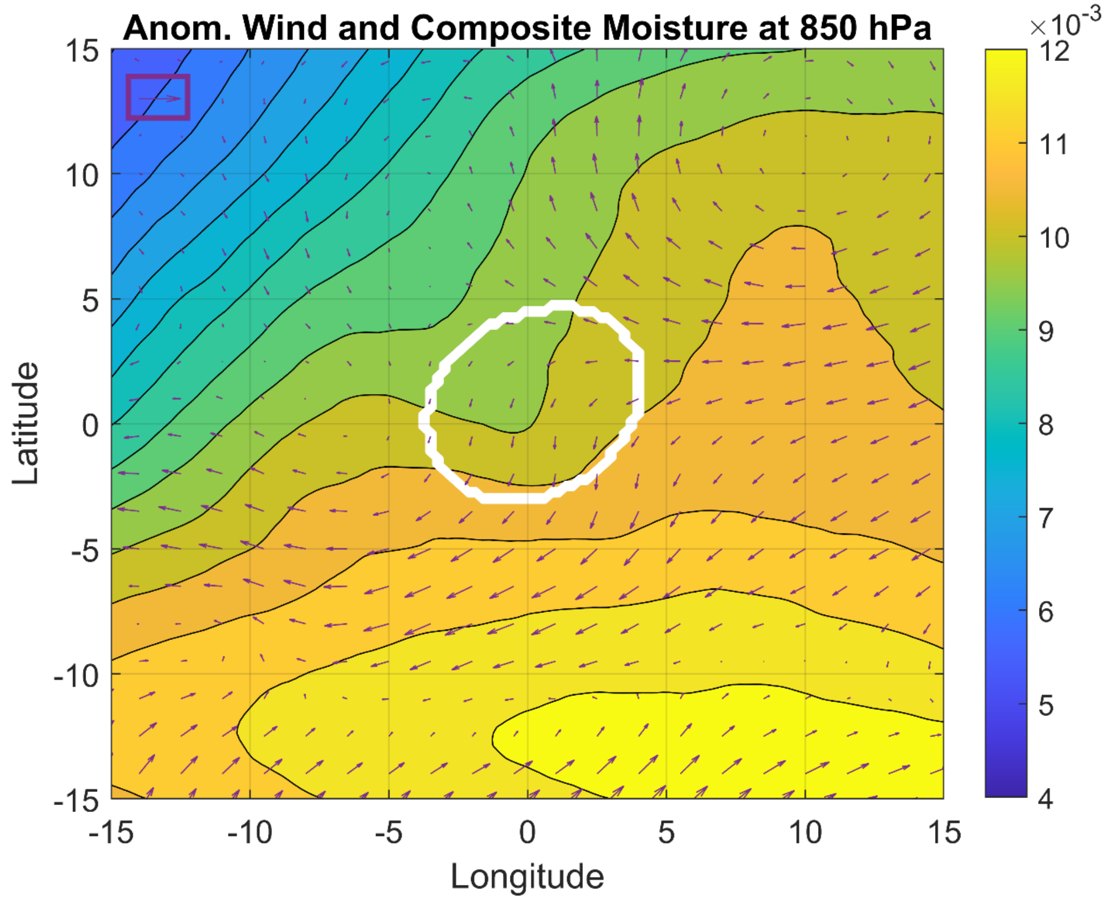

Figure 9: Composite mean anomalous winds (purple vectors) overlain on composite mean moisture mixing ratio both at 850 hPa. The magnitude of the vector in the purple box is 1 m s^{-1}. The white line outlines the 1 PVU contour at 200 hPa.

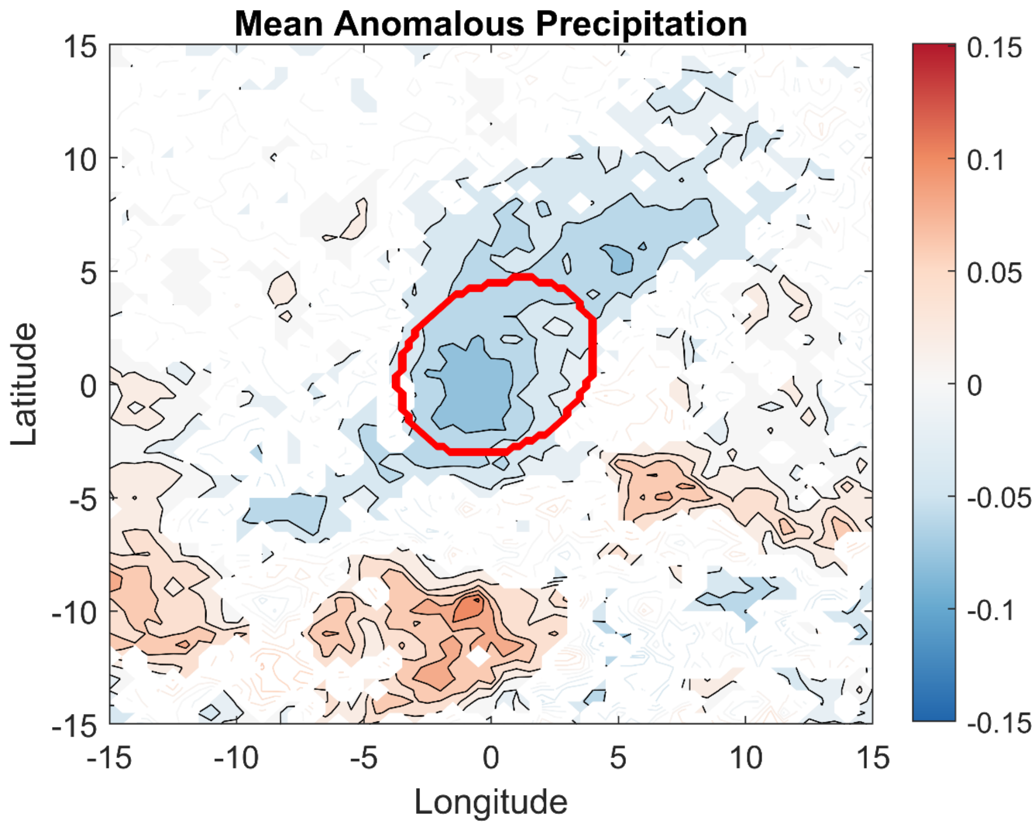

Figure 10: Spatial composites of the mean anomalous precipitation rate. Statistically significant anomalies are shown in filled contours; not-significant values are shown in open contours. The thick red line outlines the 1 PVU contour at 200 hPa.

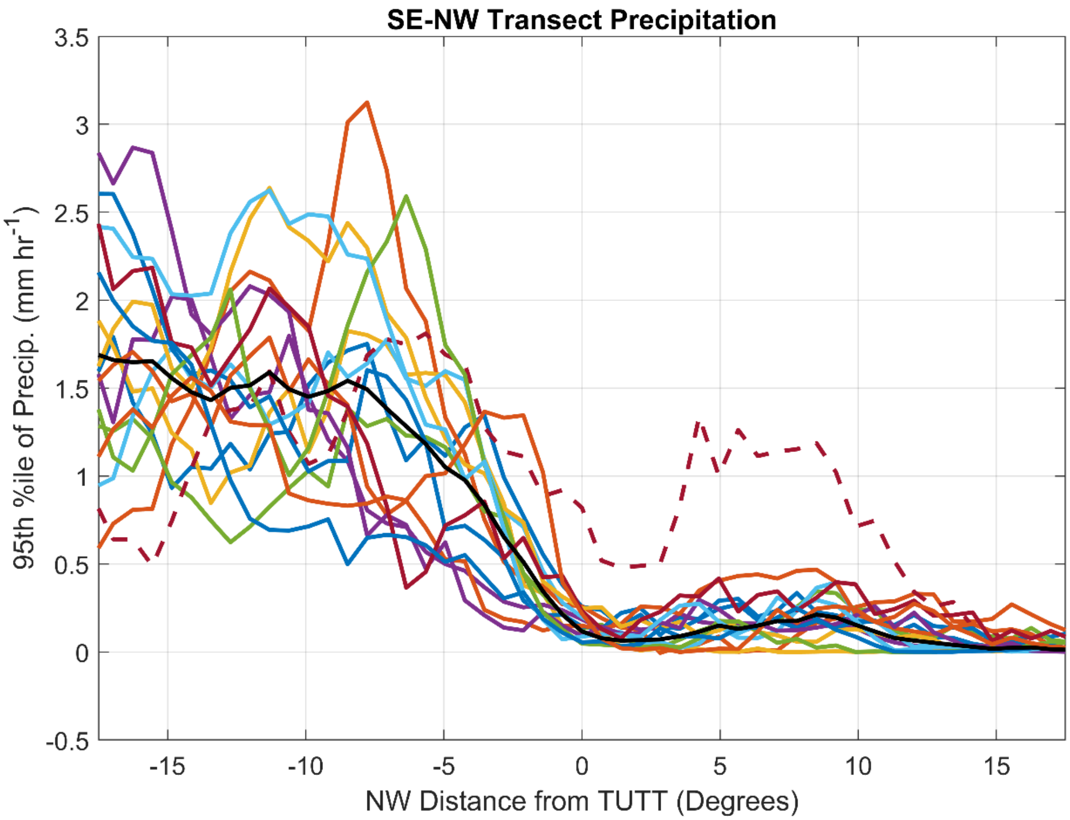

Figure 11: The 95th percentile of anomalous precipitation rate for precipitation occurring within 5° of a line running diagonally from the southeast to the northwest through the composite TUTT center. The black line is for all years. Colored lines indicate individual years. The burgundy dashed line shows data from 2004.